hep-ph/0204192
CERN–TH/2002-081
UMN–TH–2049/02
TPI–MINN–02/09

The MSSM Parameter Space with Non-Universal Higgs Masses

John Ellis[1], **Keith A. Olive**[2] and **Yudi Santoso**[2]

[1] *TH Division, CERN, Geneva, Switzerland*

[2] *Theoretical Physics Institute, University of Minnesota, Minneapolis, MN 55455, USA*

Abstract

Without assuming that Higgs masses have the same values as other scalar masses at the input GUT scale, we combine constraints on the minimal supersymmetric extension of the Standard Model (MSSM) coming from the cold dark matter density with the limits from direct searches at accelerators such as LEP, indirect measurements such as $b \to s\gamma$ decay and the anomalous magnetic moment of the muon. The requirement that Higgs masses-squared be positive at the GUT scale imposes important restrictions on the MSSM parameter space, as does the requirement that the LSP be neutral. We analyze the interplay of these constraints in the (μ, m_A), $(\mu, m_{1/2})$, $(m_{1/2}, m_0)$ and $(m_A, \tan\beta)$ planes. These exhibit new features not seen in the corresponding planes in the constrained MSSM in which universality is extended to Higgs masses.

CERN–TH/2002-081

1 Introduction

In order to avoid fine tuning to preserve the mass hierarchy $m_W \ll m_P$ [1], supersymmetry at the TeV scale is commonly postulated. Cosmology also favours the TeV mass range, if the lightest supersymmetric particle (LSP) is stable, as occurs if R parity is conserved. In the following, we work within the minimal supersymmetric extension of the Standard Model (MSSM). Furthermore, in order to satisfy the strong constraints on charged or colored dark matter[2], we require that the LSP is neutral. Over almost all of the MSSM parameter space the lightest neutral sparticle is a neutralino[1] χ, i.e., a mixture of the $\tilde{B}, \tilde{W}^3, \tilde{H}_1$ and $\tilde{H}_2$. In this case, the LSP would be an excellent candidate for astrophysical dark matter [3].

A key uncertainty in the MSSM is the pattern of soft supersymmetry breaking, as described by the scalar masses m_0, gaugino masses $m_{1/2}$ and trilinear couplings A_0 [4]. These presumably originate from physics at some high-energy scale, e.g., from some supergravity or superstring theory, and then evolve down to lower energy scale according to well-known renormalization-group equations. What is uncertain, however, is the extent to which universality applies to the scalar masses m_0 for different squark, slepton and Higgs fields, the gaugino masses $m_{1/2}$ for the $SU(3)$, $SU(2)$ and $U(1)$ gauginos, and the trilinear couplings A corresponding to different Yukawa couplings. We do not consider here non-universal gaugino masses or A parameters.

The suppression of flavour-changing neutral interactions [5] suggests that the m_0 may be universal for different matter fields with the same quantum numbers, e.g., the different squark and slepton generations [6]. However, there is no very good reason to postulate universality between, say, the spartners of left- and right-handed quarks, or between squarks and sleptons. In Grand Unified Theories (GUTs), there must be universality between fields in the same GUT multiplet, e.g., u_L, d_L, u_R and e_R in a **10** of $SU(5)$, and this would extend to all matter fields in a **16** of $SO(10)$. However, there is less reason to postulate universality between these and the Higgs fields. Nevertheless, this extension of universality to the Higgs masses (UHM) is often assumed, resulting in what is commonly termed the constrained MSSM (CMSSM). Alternatively, there may be non-universal higgs masses (NUHM) in the more general MSSM.

We and others have previously made extensive studies of the allowed parameter space in the CMSSM [7, 8, 9, 10, 11], incorporating experimental constraints and the requirement that the relic density $\Omega_\chi h^2$ fall within a range $0.1 < \Omega_\chi h^2 < 0.3$ preferred by cosmology. There have also been many studies of the NUHM case in the MSSM [12, 13, 14, 7], in which the character of the LSP may change, perhaps becoming mainly a Higgsino $\tilde{H}$, rather than a Bino $\tilde{B}$ as in the CMSSM. We think it is opportune to study the NUHM case again, taking into account more recent improvements in the understanding of the cosmological relic density $\Omega_\chi h^2$, including $\chi - \tilde{\tau}$ [10] and $\chi - \tilde{t}$ [11] coannihilations in addition to $\chi - \chi' - \chi^\pm$ coannihilations [15] and the rôles of direct-channel MSSM Higgs resonances [16, 8], as well as the (almost) final versions of the direct constraints imposed by LEP experiments.

[1] We comment below on specific cases where the sneutrino may be the LSP.

2 Experimental Constraints and the NUHM Analysis

Important experimental constraints on the MSSM parameter space are provided by direct searches at LEP, such as that on the lightest chargino $\chi^{\pm}$: $m_{\chi^{\pm}} \gtrsim 103.5$ GeV [17], and that on the selectron $\tilde{e}$: $m_{\tilde{e}} \gtrsim 99$ GeV [18], depending slightly on the other MSSM parameters. For our purposes, another important constraint is provided by the LEP lower limit on the Higgs mass: $m_H > 114$ GeV [19] in the Standard Model. This limit may be applicable to the lightest Higgs boson h in the general MSSM, although possibly in relaxed form [2]. We recall that m_h is sensitive to sparticle masses, particularly $m_{\tilde{t}}$, via loop corrections [20, 21]:

$$\delta m_h^2 \propto \frac{m_t^4}{m_W^2} \ln\left(\frac{m_{\tilde{t}}^2}{m_t^2}\right) + \ldots \tag{1}$$

which implies that the LEP Higgs limit constrains the MSSM parameters.

We also impose the constraint imposed by measurements of $b \to s\gamma$ [22], $\mathrm{BR}(B \to X_s\gamma) = (3.11 \pm 0.42 \pm 0.21) \times 10^{-4}$, which agree with the Standard Model calculation $\mathrm{BR}(B \to X_s\gamma)_{\mathrm{SM}} = (3.29 \pm 0.33) \times 10^{-4}$ [23]. Typically, the $b \to s\gamma$ constraint is more important for $\mu < 0$, but it is also relevant for $\mu > 0$, particularly when $\tan\beta$ is large.

We also take into account the anomalous magnetic moment of the muon. The BNL E821 [24] experiment reported a new measurement of $a_\mu \equiv \frac{1}{2}(g_\mu - 2)$ which deviates by 1.6 standard deviations from the best Standard Model prediction (once the pseudoscalar-meson pole part of the light-by-light scattering contribution [25] is corrected). Currently, the deviation from the Standard Model value is -6×10^{-10} to 58×10^{-10} at the 2-σ level. The 2-σ limit still prefers [26] the $\mu > 0$ part of parameter space, but $\mu < 0$ is allowed so long as either (or both) $m_{1/2}$ and m_0 are large [27]. Where appropriate, the current $g_\mu - 2$ constraint is taken into account [3].

In the following, we display the regions of MSSM parameter space where the supersymmetric relic density $\rho_\chi \equiv \Omega_\chi \rho_{critical}$ falls within the following preferred range:

$$0.1 < \Omega_\chi h^2 < 0.3. \tag{2}$$

The upper limit is rigorous, and assumes only that the age of the Universe exceeds 12 Gyr. It is also consistent with the total matter density $\Omega_m \lesssim 0.4$, and the Hubble expansion rate $h \sim 1/\sqrt{2}$ to within about 10 % (in units of 100 km/s/Mpc). An upper limit stronger than (2) could be defensible [28], in particular because global fits to cosmological data may favour a lower value of Ω_m. On the other hand, the lower limit in (2) might be weakened, in particular if there are other important contributions to the overall matter density.

In the CMSSM, the values of the Higgsino mixing parameter μ and the pseudoscalar Higgs mass m_A are determined by the electroweak vacuum conditions, once $m_{1/2}, m_0, \tan\beta$ and the trilinear supersymmetry-breaking parameter A_0 are fixed. This is no longer the case

[2] As we discuss later, there is no such relaxation in the regions of MSSM parameter space of interest to us.

[3] We note that a new experimental value with significantly reduced statistical error is expected soon, but the theoretical interpretation will still be subject to strong-interaction uncertainties in the Standard Model prediction, so the impact may be muffled.

when the universality assumption is relaxed for the Higgs multiplets. No longer assuming that the Higgs soft masses m_1 and m_2 [4] are set equal to m_0 at the GUT scale, we are free to choose μ and m_A as surrogate parameters. Thus we have as our free parameters m_0, $m_{1/2}$, A_0, $\tan\beta$, μ and m_A. The results depend somewhat on the masses of the top and bottom quarks that are assumed: for definiteness, we use the pole mass $m_t = 175$ GeV and the running mass $m_b(m_b)^{\overline{MS}}_{SM} = 4.25$ GeV.

As noted above, we include $\chi - \tilde{l}$ ($l = e, \mu, \tau$) [10] and $\chi - \tilde{t}$ [11] coannihilations in our calculation. However, since we assume for simplicity that $A_0 = 0$, $\chi - \tilde{t}$ coannihilation is not very important. Since μ is now a free parameter, the neutralino can be Bino-like or Higgsino-like depending on the ratio of μ to $m_{1/2}$. When the LSP is Higgsino-like, it is often nearly degenerate with the second lightest neutralino χ' and the lightest chargino $\chi^{\pm}$ [15]. All relevant coannihilation processes for this case, have been included. In some small regions of the parameter space χ, χ', χ^+ and $\tilde{l}$ can all be degenerate, and we have also taken into account the $\chi' - \tilde{l}$ and $\chi^{\pm} - \tilde{l}$ coannihilations.

3 Analysis of the (μ, m_A) Plane

We start our analysis by studying the range of possibilities in the (μ, m_A) plane for various fixed choices of $m_{1/2}$, m_0 and $\tan\beta$. Panel (a) of Fig. 1 displays the (μ, m_A) plane for $m_{1/2} = 300$ GeV, $m_0 = 100$ GeV and $\tan\beta = 10$. The very dark (red) regions at large $|\mu|$ appear where the LSP is no longer the neutral χ but the charged lighter stau $\tilde{\tau}_1$, which is unacceptable astrophysically. There are also small 'shark's teeth' at $|\mu| \sim 400$ GeV, $m_A \lesssim 300$ GeV where the $\tilde{\tau}_1$ is the LSP. At large $|\mu|$, the $\tilde{\tau}_1$ is driven light primarily by the large mixing term in the stau mass matrix. At small $|\mu|$, particularly at small m_A when the mass difference $m_2^2 - m_1^2$ is small, first the $\tilde{\tau}_R$ mass is driven small, making the $\tilde{\tau}_1$ the LSP again. However, at even smaller $|\mu|$ the lightest neutralino gets lighter again, since $m_\chi \simeq \mu$ when $\mu < M_1 \simeq 0.4\, m_{1/2}$.

The light (turquoise) shaded region in panel (a) of Fig. 1 is that for which $0.1 < \Omega_\chi h^2 < 0.3$. We see strips adjacent to the $\tilde{\tau}_1$ LSP regions, where $\chi - \tilde{\tau}_1$ coannihilation [10] is important in suppressing the relic density to an acceptable level. The thick cosmological region at smaller μ corresponds to the 'bulk' region familiar from CMSSM studies. The two (black) crosses indicate the position of the CMSSM points for these input parameters. Extending upward in m_A from this region, there is another light (turquoise) shaded band at smaller $|\mu|$. Here, the neutralino gets more Higgsino-like and the annihilation to W^+W^- becomes important, yielding a relic density in the allowed range [5]. For smaller $|\mu|$, the relic density becomes too small due to the $\chi - \chi' - \chi^+$ coannihilations. For even smaller $|\mu|$ ($\lesssim 30$ GeV) many channels are kinematically unavailable and we are no longer near the h and Z pole. As a result the relic density may again come into the cosmologically preferred region. However, this region is excluded by the LEP limit on the chargino mass as explained below.

[4] The Higgs multiplets $H_{1,2}$ couple to d, u quarks, respectively.

[5] This is similar to the focus-point region [29] in the CMSSM.

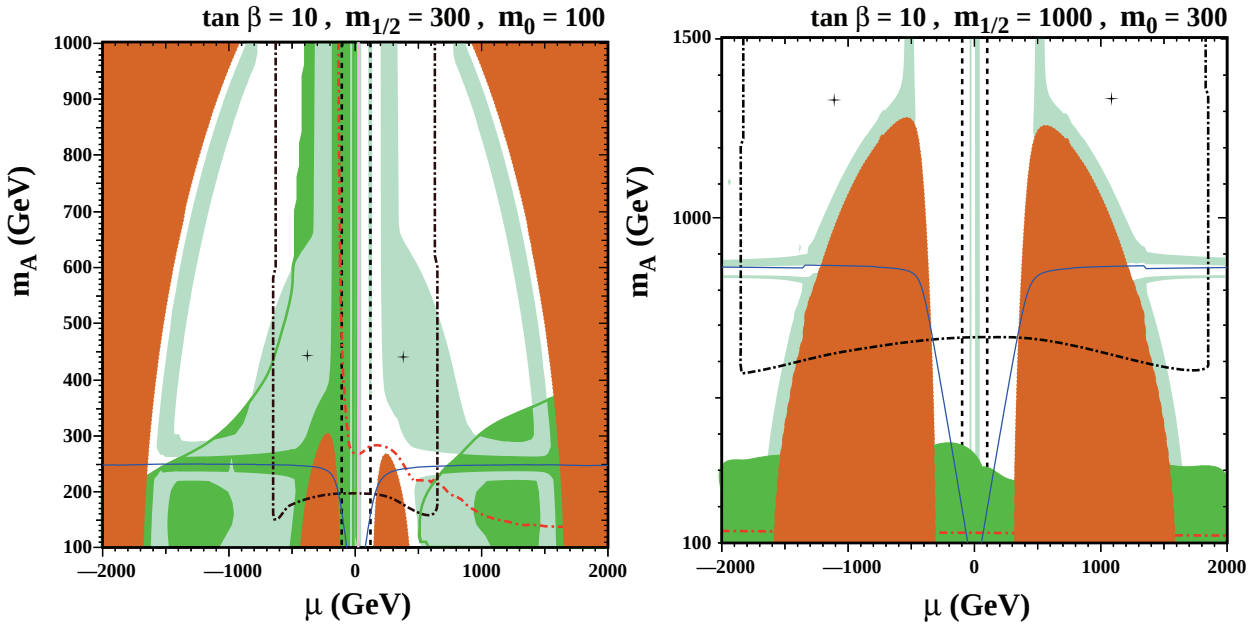

Figure 1: *Compilations of phenomenological constraints on the MSSM with NUHM in the* (μ, m_A) *plane for* $\tan\beta = 10$ *and (a)* $m_0 = 100$ *GeV,* $m_{1/2} = 300$ *GeV, (b)* $m_0 = 300$ *GeV,* $m_{1/2} = 1000$ *GeV, assuming* $A_0 = 0$, $m_t = 175$ *GeV and* $m_b(m_b)^{\overline{MS}}_{SM} = 4.25$ *GeV. The light (turquoise) shading denotes the region where* $0.1 < \Omega_\chi h^2 < 0.3$, *and the (blue) solid line is the contour* $m_\chi = m_A/2$, *near which rapid direct-channel annihilation suppresses the relic density. The darker (green) shading shows the impact of the* $b \to s\gamma$ *constraint, and the darkest (red) shading shows where the LSP is charged. The dark (black) dashed line is the chargino constraint* $m_{\chi^\pm} > 104$ *GeV: lower* $|\mu|$ *values are not allowed. The lighter (red) dot-dashed line is the contour* $m_h = 114$ *GeV calculated using* `FeynHiggs` *[21]: lower* m_A *values are not allowed. The dark (black) dot-dashed line indicates when one or another Higgs mass-squared becomes negative at the GUT scale: only lower* $|\mu|$ *and larger* m_A *values are allowed. The crosses denote the values of* μ *and* m_A *found in the CMSSM.*

The unshaded regions between the allowed bands have a relic density that is too high: $\Omega_\chi h^2 > 0.3$. However, the $\tilde{\tau}$ coannihilation and bulk bands are connected by horizontal bands of acceptable relic density that are themselves separated by unshaded regions of low relic density, threaded by solid (blue) lines asymptoting to $m_A \sim 250$ GeV. These lines correspond to cases when $m_\chi \simeq m_A/2$, where direct-channel annihilation: $\chi + \chi \to A, H$ is important, and suppresses the relic density [8, 16] creating 'funnel'-like regions.

Overlaying the cosmological regions are dark (green) shaded regions excluded by $b \to s\gamma$. That for $\mu < 0$ is more important, as expected from previous analyses. Taking this into account, most of the bulk and coannihilation regions are allowed for $\mu > 0$, but only the coannihilation regions and a small slice of the bulk region for $\mu < 0$. In this example, the 'funnel' regions are largely excluded by $b \to s\gamma$ for both signs of μ.

We next explain the various contours shown in Fig. 1. The dark (black) dashed line in Fig. 1(a) is the contour $m_{\chi^\pm} = 104$ GeV, representing the LEP kinematic limit on the chargino mass. The actual LEP lower limit is in fact generally somewhat smaller than this,

depending on the details of the MSSM parameters, but the differences would be invisible on this plot. We see that the chargino constraint excludes the $|\mu| \lesssim 100$ GeV strip. The lighter (red) dot-dashed line in Fig. 1(a) is the LEP lower limit of 114 GeV on the mass of the lightest MSSM Higgs boson h, as calculated using the `FeynHiggs` programme [21]. This limit is relaxed in certain regions of parameter space because of a suppression of the ZZh coupling but, as discussed below in connection with Fig. 2, this relaxation is irrelevant for the conclusions presented here. For the choices of the other MSSM parameters in Fig. 1(a), the main effect of the Higgs constraint is essentially to exclude negative values of μ. The pale (pink) solid line at $\mu = 0$ marks the $g_\mu - 2$ constraint. This constraint excludes the $\mu < 0$ half-plane, while allowing all of the $\mu > 0$ parameter space for this particular choice of $m_{1/2}$ and m_0.

The darker (black) dot-dashed line in Fig. 1(a) indicates where one or the other of the Higgs mass-squared becomes negative at the input GUT scale, specifically when either $(m_1^2 + \mu^2) < 0$ or $(m_2^2 + \mu^2) < 0$. One could argue that larger values of $|\mu|$ and/or smaller values of m_A are excluded by requiring the preferred electroweak vacuum to be energetically favoured and not bypassed early in the evolution of the Universe. However, for a different point of view, see [30].

As noted above, the two (black) crosses in Fig. 1(a) are the two pairs $(\mu, m_A) \simeq (\pm 390, 450)$ GeV obtained in the CMSSM, assuming that the soft supersymmetry-breaking Higgs scalar masses are equal to the universal squark and slepton masses-squared at the GUT input scale (UHM). For this particular choice of the other MSSM parameters $m_{1/2}, m_0, A_0$ and $\tan\beta$, these two CMSSM points both yield relic densities $\Omega_\chi h^2 = 0.21$, within the range preferred by astrophysics and cosmology. On the other hand, the CMSSM point with $\mu < 0$ has unacceptable values for $b \to s\gamma$ decay, a_μ, and m_h, although the latter might conceivably be salvaged if the theoretical approximations in `FeynHiggs` happen to err in the favourable direction.

The main conclusions from Fig. 1(a) are that moderate values of $\mu > 0$ are favoured, m_A cannot be small, and there is a large fraction of the remaining MSSM parameter space where the cosmological relic density lies within the range favoured by astrophysics and cosmology. This includes parts of the 'bulk' regions identified in CMSSM studies, with 200 GeV $\lesssim \mu \lesssim$ 1000 GeV and 270 GeV $\lesssim m_A \lesssim$ 650 GeV, generalizing the CMSSM point for $\mu > 0$.

The notations used for the constraints illustrated in the other panel of Fig. 1 are the same, but the constraints interplay in different ways. In panel (b), we have chosen a larger value of $m_{1/2}$. In this case, the previous region excluded by the neutral LSP constraint at large $|\mu|$, migrates to larger $|\mu|$ and is no longer visible in this panel. However, the 'shark's teeth' for moderate $|\mu|$ grow, reaching up to $m_A \sim 1250$ GeV. These arise when one combines a large value of $m_{1/2}$ with a relatively small value of m_0, and one may find a $\tilde{\tau}$ or even a $\tilde{e}$ LSP. The large value of $m_{1/2}$ also keeps the rate of $b \to s\gamma$ under control unless m_A is very small. The chargino constraint is similar to that in panel (a), whereas the m_h constraint is irrelevant due to the large value of $m_{1/2}$. The $g_\mu - 2$ constraint does not provide any exclusion here. Finally, we observe that the GUT mass-squared positivity constraint now allows larger values of $|\mu| \lesssim 1800$ GeV. In this example, the two CMSSM points are at

$(\mu, m_A) \simeq (\pm 1100, 1330)$ GeV and both have relic densities that are too large: $\Omega_\chi h^2 \simeq 1.15$.

The main conclusions from Fig. 1(b) are that moderate values of μ are favoured, which may be of either sign, but still m_A cannot be small. As in panel (a), there is a large fraction of the remaining MSSM parameter space where the cosmological relic density lies within the range favoured by astrophysics and cosmology, for both signs of μ.

The reader may be wondering by now: how non-universal are the Higgs masses in the previous plots? Do they differ only slightly from universality - in which case the usual CMSSM results would be very *unstable* numerically, or do they involve violations of universality by orders of magnitude - in which case the NUHM discussion would be unimportant and the usual CMSSM results would be very *stable* numerically? Some answers are provided in Fig. 2, where we plot contours of $\hat{m}_1 \equiv \mathrm{sign}(m_1^2) \times |m_1/m_0|$ as paler (red) curves and of $\hat{m}_2 \equiv \mathrm{sign}(m_2^2) \times |m_2/m_0|$ as darker (black) curves. We see in panel (a), for $\tan\beta = 10$, $m_{1/2} = 300$, $m_0 = 100$ GeV and $A_0 = 0$, corresponding to panel (a) of Fig. 1, that relatively large values are attained for both $\hat{m}_1$ and $\hat{m}_2$, ranging up to 15 or more in modulus. However, comparing Fig. 1(a) and Fig. 2(a), we see that such large values are not attained in the restricted region of the (μ, m_A) plane that are allowed by the various phenomenological constraints discussed earlier. We have indicated by darker shading the regions of Fig. 2(a) which are allowed by the non-cosmological constraints, and see that $|\hat{m}_{1,2}| \lesssim 5$ in the regions allowed.

Turning now to panel (b) of Fig. 2, for $\tan\beta = 10$, $m_{1/2} = 1000$, $m_0 = 300$ GeV and $A_0 = 0$, we see values of $|\hat{m}_{1,2}| \lesssim 5$ throughout the portion of the plane displayed. Comparing again with the corresponding panel (b) of Fig. 1, we see that most of the displayed range of μ is allowed by the experimental constraints, but only for $m_A \gtrsim 600$ GeV. In this region, we find $|\hat{m}_{1,2}| \lesssim 5$.

We conclude that the answer to the questions posed earlier lie in between the extremes proposed. The variations in $|\hat{m}_{1,2}|$ are by no means negligible, but neither are they excessive within the regions of parameter space allowed by the experimental constraints. The CMSSM results are not excessively unstable, but significant variations are possible for plausible ranges of $\hat{m}_{1,2}$.

We comment finally on the magnitude of the ZZh coupling $\sin^2(\beta-\alpha)$, which controls the observability of the lightest MSSM Higgs boson at LEP. The contours $\sin^2(\beta-\alpha) = 0.7, 0.5$ and 0.3 are shown as closely-spaced dashed lines at the bottom of each panel in Fig. 2. In the bulk of the (μ, m_A) planes shown, the ZZh coupling is close to its Standard Model value, and the LEP lower limit on m_h is indistinguishable from the Standard Model value limit of 114 GeV.

4 Analysis of the (μ, M_2) Plane

We now turn to projections of the MSSM parameter space on the (μ, M_2) plane, which is often used in the analysis of the chargino and neutralino sectors of the MSSM. In the past, it has been demonstrated how the cosmological constraint on the relic neutralino density may be satisfied in a large part of the (μ, M_2) plane, for certain values of the other MSSM

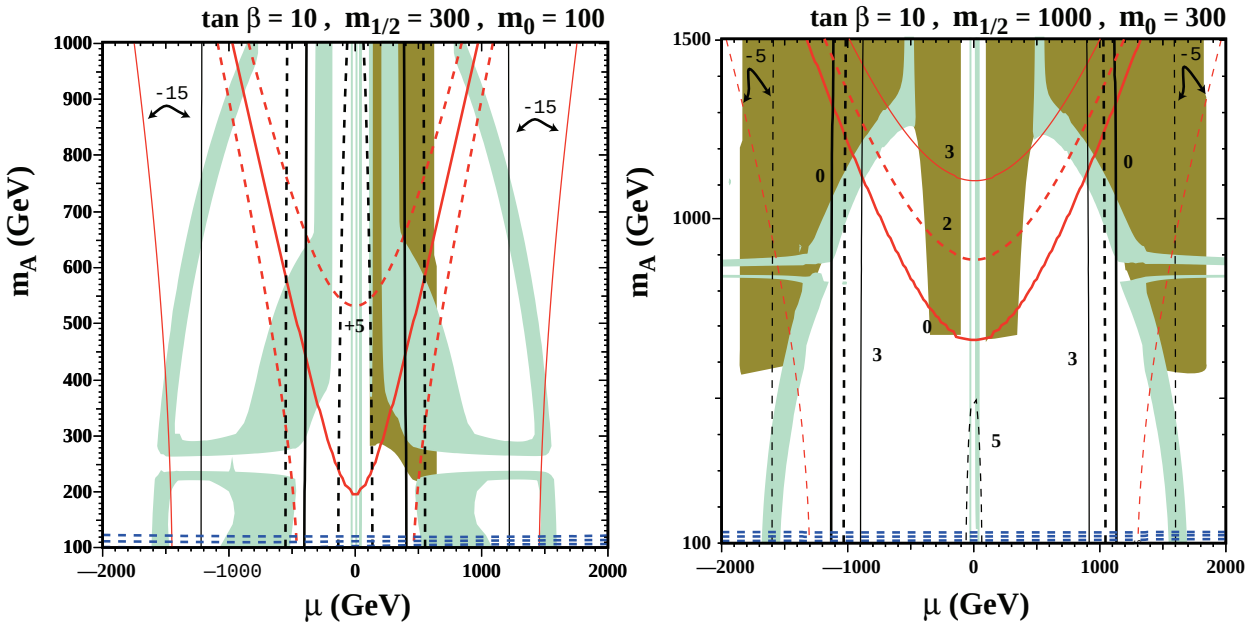

Figure 2: *Contours of the scaled Higgs masses* $\hat{m}_1$ *and* $\hat{m}_2$ *in the* (μ, m_A) *plane for* $\tan\beta = 10$ *and (a)* $m_0 = 100$ *GeV,* $m_{1/2} = 300$ *GeV, (b)* $m_0 = 300$ *GeV,* $m_{1/2} = 1000$ *GeV, assuming* $A_0 = 0$, $m_t = 175$ *GeV and* $m_b(m_b)^{\overline{MS}}_{SM} = 4.25$ *GeV. As in Fig. 1, the light (turquoise) shading denotes the region where* $0.1 < \Omega_\chi h^2 < 0.3$. *The darker shading denotes the region not excluded by the other constraints. The dark (black) lines correspond to contours of* $\hat{m}_2$, *and the lighter (red) lines to contours of* $\hat{m}_1$. *In (a) the thick solid contours correspond to* $\hat{m} = 0$, *the thick dashed contours to* $\hat{m} = \pm 5$, *and the thin solid contours to* $\hat{m} = -15$. *In (b) the thick solid contours correspond to* $\hat{m} = 0$, *the thick dashed contours to* $\hat{m} = 2$, *the thin solid contours to* $\hat{m} = 3$, *and the thin dashed contours to* $\hat{m} = \pm 5$. *The dark (blue) dashed lines at very low values of* m_A *indicate the contours* $\sin^2(\beta - \alpha) = 0.7, 0.5$ *and* 0.3, *which decrease with* m_A.

parameters [12, 13, 14, 7]. Here we limit ourselves to a couple of examples that indicate how the cosmological region may vary.

Panel (a) of Fig. 3 displays the (μ, M_2) plane for the choices $\tan\beta = 10$, $m_0 = 100$ GeV, $m_A = 700$ GeV and $A_0 = 0$. In this case, the region favoured by cosmology, shown by the light (turquoise) shading, is in the part of the plane where the LSP χ is mainly a Bino, as preferred in the CMSSM. The LEP chargino constraint, shown as a dark (black) dashed line, excludes small values of μ and/or M_2, where a Higgsino LSP might have constituted the dark matter. The m_h constraint, shown as a paler (red) dot-dashed line, excludes low values of M_2, particularly for $\mu < 0$, but allows substantial fractions of the cosmological regions. The $b \to s\gamma$ constraint, shown in darker shading, excludes another part of the remaining allowed region for $\mu < 0$, but leaves almost untouched the allowed region for $\mu > 0$. The $g_\mu - 2$ constraint, shown as a pale (pink) solid line, excludes a larger region of $\mu < 0$, but leaves an allowed region at higher M_2. The requirement that the effective Higgs masses-squared be positive at the GUT scale allows a triangular region centred around $\mu = 0$ and extending up to $M_2 \sim 900$ GeV, bounded by the dark (black) dot-dashed lines, and is compatible with all the other constraints in regions with both signs of μ. The cosmological region is bounded above by the dark (red) shaded region where the LSP is charged, close to which coannihilation is important in suppressing the relic density to an acceptable level. Also shown at large M_2 is the solid (blue) line where $m_\chi = m_A/2$, but this has little effect on the relic density in the region allowed by the other constraints.

Panel (b) of Fig. 3 displays the (μ, M_2) plane for the choices $\tan\beta = 10, m_0 = 400$ GeV, $m_A = 700$ GeV and $A_0 = 0$. In this case, the cosmological region is largely complementary to panel (a), since both the Bino and Higgsino regions are excluded. Only narrow strips in the regions where the LSP is a strong mixture of gaugino and Higgsino have an acceptable relic density, with the exception of indentations where $m_\chi \sim m_A/2$ and broader regions at large M_2, where contributions from s-channel annihilation and $\tilde{\tau}$ coannihilation are both important. The chargino, Higgs, $b \to s\gamma$, $g_\mu - 2$ and GUT positivity constraints interplay much as in panel (a).

We have also examined the (μ, M_2) planes for other choices of m_0 and m_A. With a judicious choice of these parameters, a large fraction of the domain where $\mu \gtrsim M_2$ and the LSP is gaugino-like may happen to have an acceptable relic density, though it may then be excluded by other constraints. However, we have not found any instance where a mainly Higgsino-like LSP is permitted with a sufficiently large relic density: see also [14]. This is largely due to the LEP lower limit on $m_{\chi^\pm}$ and the fact that large M_2 is excluded at small $|\mu|$ by the neutral LSP requirement.

5 Analysis of the $(m_{1/2}, m_0)$ Plane

This projection of the MSSM parameter space has often been used in studies of supersymmetric dark matter, in particular in the context of the CMSSM, where it was instrumental in the specification [31] of benchmark scenarios compatible with all the experimental and cosmological constraints discussed earlier. Here we discuss examples in the more general MSSM context, which indicate some of the range of new possibilities that it opens up.

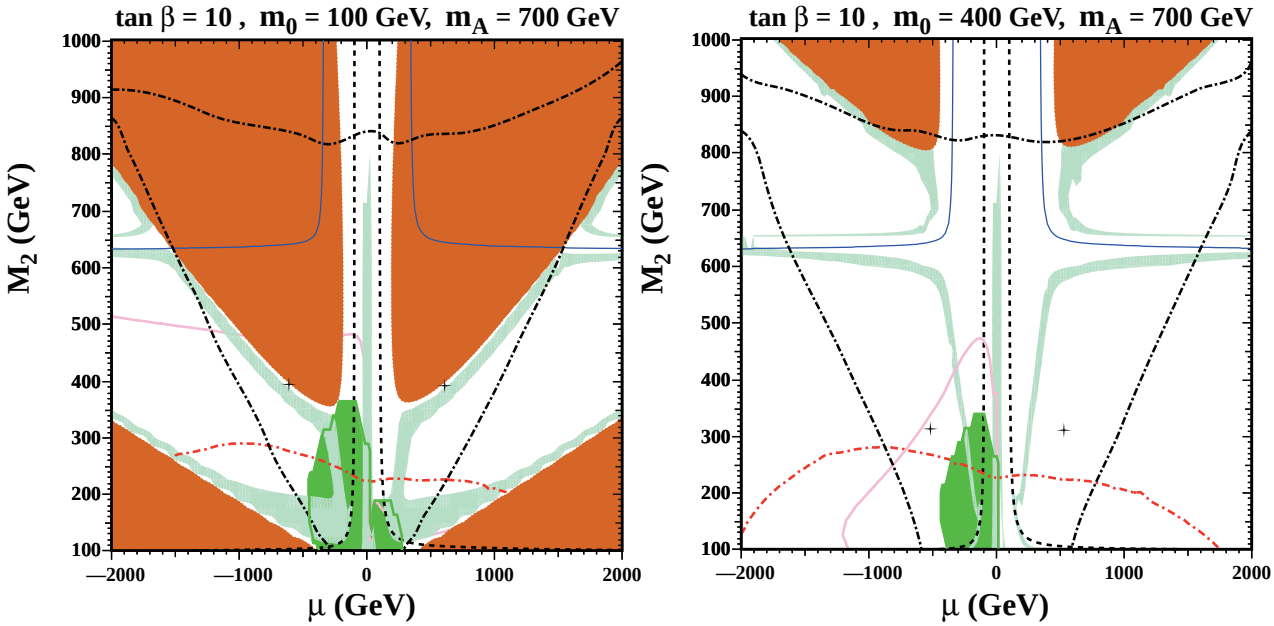

Figure 3: *Compilations of phenomenological constraints on the MSSM with NUHM in the* (μ, M_2) *plane for* $\tan\beta = 10$ *and (a)* $m_0 = 100$ *GeV,* $m_A = 700$ *GeV, (b)* $m_0 = 400$ *GeV,* $m_A = 700$ *GeV, again assuming* $A_0 = 0$, $m_t = 175$ *GeV and* $m_b(m_b)^{\overline{MS}}_{SM} = 4.25$ *GeV. The pale (turquoise) shading denotes the region where* $0.1 < \Omega_\chi h^2 < 0.3$, *and the (blue) solid line is the contour* $m_\chi = m_A/2$, *near which rapid direct-channel annihilation suppresses the relic density. The darker (green) shading shows the impact of the* $b \to s\gamma$ *constraint, and the darkest (red) shading shows where the LSP is charged. The dark (black) dashed line is the chargino constraint* $m_{\chi^\pm} > 104$ *GeV: lower values of* $|\mu|$ *and/or* M_2 *are not allowed. The lighter (red) dot-dashed line is the contour* $m_h = 114$ *GeV calculated using* `FeynHiggs` *[21]: lower* m_A *are not allowed. The pale (pink) solid line shows the region excluded by* $g_\mu - 2$. *The dark (black) dot-dashed triangular line indicates when one or another Higgs mass-squared becomes negative at the GUT scale: only lower* $|\mu|$ *and intermediate* $m_{1/2}$ *are allowed. The (black) crosses denote the CMSSM points.*

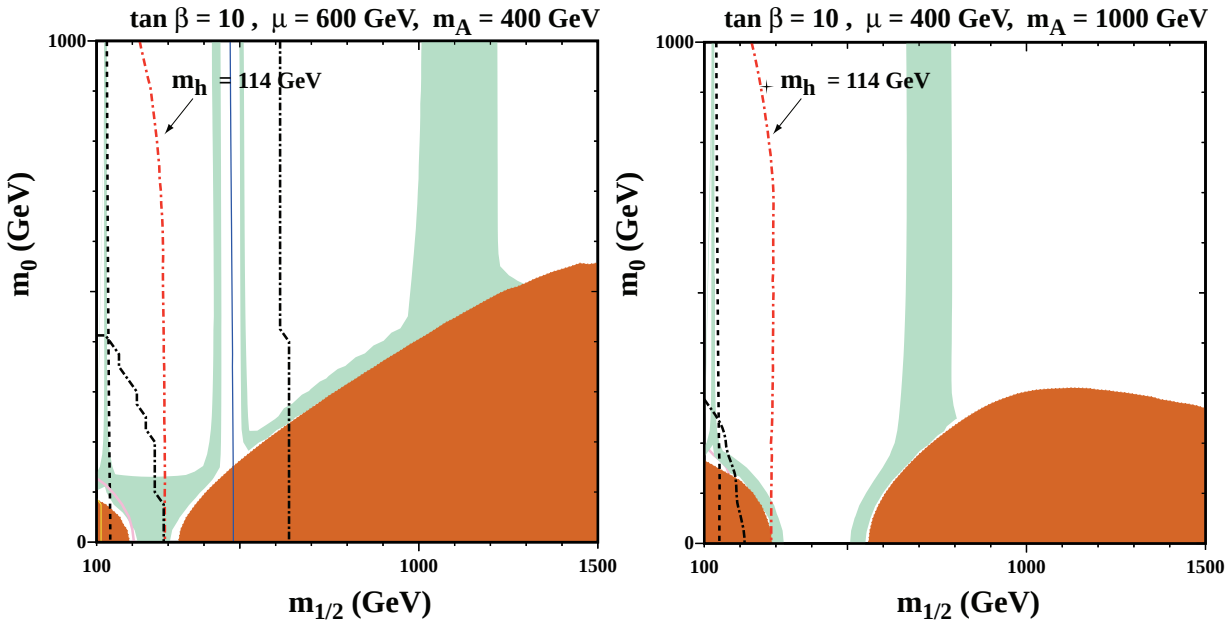

Figure 4: *Compilations of phenomenological constraints on the MSSM with NUHM in the* $(m_{1/2}, m_0)$ *plane for* $\tan\beta = 10$ *and (a)* $\mu = 600$ *GeV,* $m_A = 400$ *GeV, (b)* $\mu = 400$ *GeV,* $m_A = 1000$ *GeV, again assuming* $A_0 = 0$, $m_t = 175$ *GeV and* $m_b(m_b)^{\overline{MS}}_{SM} = 4.25$ *GeV. The pale (turquoise) shading denotes the region where* $0.1 < \Omega_\chi h^2 < 0.3$, *and the (blue) solid line is the contour* $m_\chi = m_A/2$, *near which rapid direct-channel annihilation suppresses the relic density. The darkest (red) shading shows where the LSP is charged. The dark (black) dashed line is the chargino constraint* $m_{\chi^\pm} > 104$ *GeV: lower* $m_{1/2}$ *are not allowed. The lighter (red) dot-dashed line is the contour* $m_h = 114$ *GeV calculated using* `FeynHiggs` *[21]: lower* $m_{1/2}$ *are not allowed. The light (pink) solid line is where the supersymmetric contribution to the muon anomalous moment is* $a_\mu = 58 \times 10^{-10}$*: lower* m_0 *and* $m_{1/2}$ *are excluded at the* $2-\sigma$ *level. The dark (black) dot-dashed lines indicates when one or another Higgs mass-squared becomes negative at the GUT scale: only intermediate values of* $m_{1/2}$ *are allowed in panel (a), and larger values in (b). The (black) cross in panel (b) denotes the CMSSM point.*

Panel (a) of Fig. 4 shows the $(m_{1/2}, m_0)$ plane for $\tan\beta = 10$ and the particular choices $\mu = 600$ GeV and $m_A = 400$ GeV. The dark (red) shaded regions are excluded because the LSP is charged: the larger part resembles the similar excluded regions in the CMSSM. As in the CMSSM studies, there are light (turquoise) shaded strips close to these forbidden regions where coannihilation suppresses the relic density sufficiently to be cosmologically acceptable. Further away from these regions, the relic density is generally too high. The near-vertical dark (black) dashed and light (red) dot-dashed lines are the LEP exclusion contours $m_{\chi^\pm} > 104$ GeV and $m_h > 114$ GeV. As in the CMSSM case, they exclude low values of $m_{1/2}$, and hence rule out rapid relic annihilation via direct-channel h and Z^0 poles.

A striking feature when $m_{1/2} \sim 400$ to 500 GeV is a 'funnel' with a double strip of acceptable relic density. This is due to rapid annihilation via the direct-channel A, H poles which occur when $m_\chi = m_A/2 = 200$ GeV, indicated by the solid (blue) line. Inside the shaded double strip, the funnel contains an unshaded strip where the relic density falls below

the range preferred by cosmology in the absence of other types of cold dark matter. The existence of analogous rapid-annihilation funnels has been noticed previously in the CMSSM context: there they were diagonal in the $(m_{1/2}, m_0)$ plane, because the CMSSM imposes a link between m_0 and m_A that is absent in the more general MSSM discussed here.

There is also another strip in Fig. 4(a) around $m_{1/2} \sim 1100$ GeV where the relic density falls again into the allowed range. In this region, the neutralino acquires enough Higgsino content for the relic density be in the range preferred by cosmology. For larger $m_{1/2}$, the relic density is suppressed even more by $\chi - \chi' - \chi^\pm$ coannihilation, and for $m_{1/2} \gtrsim 1200$ GeV the relic density falls down below 0.1. This strip along with most of the $(m_{1/2}, m_0)$ plane shown in Fig. 4(a) is actually excluded by the requirement that the Higgs scalar masses be positive at the input GUT scale, as indicated by the dark (black) dot-dashed lines. However, the rapid-annihilation funnel is still allowed by this constraint, as is a part of the $\chi - \tilde{\ell}$ coannihilation region. The CMSSM point is located beyond the region shown here.

Panel (b) of Fig. 4 shows the $(m_{1/2}, m_0)$ plane for $\tan\beta = 10$ and the different choices $\mu = 400$ GeV and $m_A = 1000$ GeV. In this case, the dark (red) shaded charged-LSP region has rather different shape, but still excludes a substantial region with large $m_{1/2}$ and small m_0. The striking feature of Fig. 4(b) is the broad band of allowed relic density around $m_{1/2} \sim 700$ GeV, where the relic density is suppressed into the preferred range by $\chi - \chi' - \chi^\pm$ coannihilation, the relic density falling below 0.1 for $m_{1/2} \gtrsim 800$ GeV. In this case, the region allowed by the GUT stability requirement extends up to $m_{1/2} \sim 1600$ GeV, and is therefore satisfied throughout most of the displayed part of the $(m_{1/2}, m_0)$ plane.

In the small $m_0 \lesssim 200$ GeV and $m_{1/2} \lesssim 300$ GeV corner, the tau sneutrino can become lighter than the stau, due to the negative value of $m_2^2 - m_1^2$. Including $\chi - \tilde{\nu}_\tau$ coannihilation would shift the region preferred by cosmology for the χ LSP to somewhat higher values of m_0 and $m_{1/2}$. Note that, in a very narrow strip between the χ- and $\tilde{\tau}$-LSP regions, the LSP is in fact $\tilde{\nu}_\tau$. The direct-channel H, A rapid-annihilation region is not seen in panel (b), because the neutralino has already become Higgsino-like with a mass ~ 400 GeV when $m_{1/2} \sim 1000$ GeV, and therefore m_χ is always below $m_A/2$. For other MSSM choices, the rapid-annihilation region may overlap with the broad band where $\chi - \chi' - \chi^\pm$ coannihilation begins to become important.

These two examples serve to demonstrate that the $(m_{1/2}, m_0)$ plane may look rather different in the CMSSM from its appearance in the CMSSM for the same value of $\tan\beta$. In particular, the locations of rapid-annihilation funnels and $\chi - \chi' - \chi^\pm$ coannihilation regions are quite model-dependent, and the GUT stability requirement may exclude large parts of the $(m_{1/2}, m_0)$ plane.

6 Analysis of the $(m_A, \tan\beta)$ Plane

This projection of the MSSM parameter space is often used in discussions of Higgs phenomenology, and a number of benchmark Higgs scenarios have been proposed [32]. As we now see in more detail, these do not always take fully into account other phenomenological constraints on the MSSM. We give examples of $(m_A, \tan\beta)$ planes for selected values of the

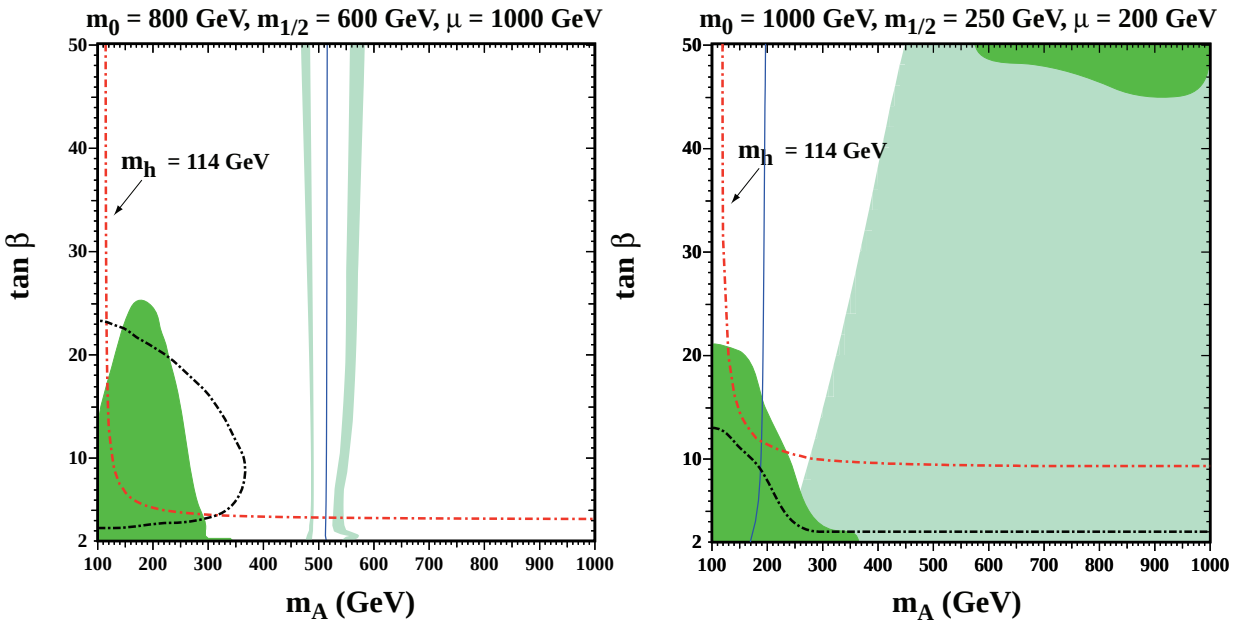

Figure 5: *Compilations of phenomenological constraints on the MSSM with NUHM in the* $(m_A, \tan\beta)$ *plane for* $(m_{1/2}, m_0, \mu) =$ (a)$(600, 800, 1000)$, (b)$(250, 1000, 200)$ *GeV. The lighter (red) dot-dashed lines are the contours* $m_h = 114$ *GeV, the solid (blue) lines show where* $m_\chi \sim m_A/2$ *and the dark (black) dot-dashed line indicates when one or another Higgs mass-squared becomes negative at the GUT scale. The light (turquoise) shading indicates where* $0.1 < \Omega_\chi h^2 < 0.3$*, the darker (green) shaded regions are excluded by the* $b \to s\gamma$ *constraint.*

other MSSM parameters in Fig. 5. We first note the following general features. The LEP constraint on m_h excludes a region at low m_A and/or $\tan\beta$, and the $b \to s\gamma$ constraint also removes large domains of the $(m_A, \tan\beta)$ planes, whose locations depend on the other MSSM parameters. The requirement that the Higgs masses-squared be positive at the GUT scale also excludes large domains of parameter space. However, the most striking constraint is that imposed by the cosmological relic density.

We discuss first panel (a) of Fig. 5, for $(m_{1/2}, m_0, \mu) = (600, 800, 1000)$ GeV. This is similar to one of the Higgs benchmark scenarios proposed in [32], which has $\mu = 2000$ GeV. However, we find that, for such a large value of μ, the GUT positivity constraints would be disobeyed all over the $(m_A, \tan\beta)$ plane. This reflects the fact the good renormalization-group running up to the GUT scale was not considered as a criterion in selecting the Higgs benchmark points. Reducing μ to the value 1000 GeV shown in panel (a) of Fig. 5, the GUT positivity constraints exclude a region at small m_A and $\tan\beta$, which is largely excluded also by the $b \to s\gamma$ constraint. In this panel, there is only a very narrow range of values of m_A where the relic density falls within the range favoured by cosmology. It corresponds to one of the 'funnels' noted previously in an analysis of the CMSSM at large $\tan\beta$ [8], and is actually divided into two strips. The broader strip of m_A values is just above $m_A \sim 2m_\chi$, and a narrower strip appears just below $m_A \sim 2m_\chi$. In between, there is a narrow strip of m_A values where the relic density lies below the preferred cosmological range: this strip would

be allowed if there is another important source of cold dark matter. Outside the double strip around $m_A \sim 2m_\chi$, the relic density is higher than allowed by cosmology. This exclusion could be evaded only by postulating that the lightest neutralino is unstable, either in an R-conserving model if there is a lighter sparticle such as the gravitino, or in an R-violating model. Thus most of the plane in panel (a) of Fig. 5 is excluded, even after reducing μ.

The picture changes strikingly in panel (b) of Fig. 5, for the choices $(m_{1/2}, m_0, \mu) = (250, 1000, 200)$ GeV. The contour $m_h = 114$ GeV is shown as a lighter (red) dot-dashed line descending steeply when $m_A \sim 130$ GeV, and then flattening out at $\tan\beta \sim 10$. The vertical solid (red) line shows where $m_\chi \sim m_A/2$. The dark (green) shaded regions at $(m_A, \tan\beta) \lesssim (300 \text{ GeV}, 20)$ and $\gtrsim (600 \text{ GeV}, 45)$ are excluded by the $b \to s\gamma$ constraint. We see in this case that the relic density constraint, indicated by the light (turquoise) shading, is satisfied throughout a broad swathe of $m_A \gtrsim 250$ GeV for $\tan\beta = 5$ to $m_A \gtrsim 450$ GeV for $\tan\beta = 50$. The requirement that the Higgs masses-squared be positive at the GUT scale excludes a domain of parameter space at low $\tan\beta$, as indicated by the dark dot-dashed line.

The Higgs benchmark scenarios were not chosen with the cosmological relic density in mind, whereas this was taken explicitly into account in formulating the sparticle benchmark scenarios proposed in [31]. It would be interesting to study NUHM Higgs benchmark scenarios that respect the cosmological relic density constraint more systematically. This could perhaps be done by postulating a value of $m_{1/2}$ that varies with $\tan\beta$. However, a detailed study of this point goes beyond the scope of this paper.

7 Conclusions

We have shown in this paper that relaxing the scalar-mass universality assumption for the MSSM Higgs multiplets opens up many phenomenological possibilities that were not evident in CMSSM studies with universal masses. We have emphasized the importance of requiring the LSP to be neutral and imposing the positivity of scalar masses-squared at the GUT scale. We find that a mainly Bino neutralino LSP is still preferred, though it may also be mixed with a large Higgsino component. However, we do not find MSSM parameter regions where the LSP is mainly a Higgsino. In addition to direct-channel A, H poles and $\chi - \tilde{\ell}$ coannihilation, we have identified generic instances where $\chi - \chi' - \chi^\pm$ coannihilation is important. We have also shown that Higgs benchmark scenarios do not respect in general the full range of phenomenological requirements. It is desirable to look for an agreed set of MSSM benchmarks that incorporate these in the studies of Higgs phenomenology, which we do not attempt here.

The higher-dimensional parameter space of the MSSM with non-universal Higgs masses is clearly much richer than the simplified CMSSM, and we have only been able to touch on a few of the more striking aspects in this paper. More work is needed to digest more fully the impacts of the different experimental, phenomenological, theoretical and cosmological constraints. There are surely many more interesting features beyond those mentioned here.

Acknowledgments

We thank Toby Falk for many valuable discussions. The work of K.A.O. and Y.S. was supported partly by DOE grant DE–FG02–94ER–40823.

References

[1] L. Maiani, *Proceedings of the 1979 Gif-sur-Yvette Summer School On Particle Physics*, 1; G. 't Hooft, in *Recent Developments in Gauge Theories, Proceedings of the Nato Advanced Study Institute, Cargese, 1979*, eds. G. 't Hooft *et al.*, (Plenum Press, NY, 1980); E. Witten, Phys. Lett. B **105** (1981) 267.

[2] J. Rich, M. Spiro and J. Lloyd-Owen, Phys. Rep. **151**, 239 (1987);
P.F. Smith, Contemp. Phys. **29**, 159 (1998);
T.K. Hemmick et al., Phys. Rev. **D41**, 2074 (1990).

[3] J. Ellis, J.S. Hagelin, D.V. Nanopoulos, K.A. Olive and M. Srednicki, Nucl. Phys. B **238** (1984) 453; see also H. Goldberg, Phys. Rev. Lett. **50** (1983) 1419.

[4] S. Dimopoulos and H. Georgi, Nucl. Phys. B **193** (1981) 150; N. Sakai, Z. Phys. C **11** (1981) 153.

[5] J. R. Ellis and D. V. Nanopoulos, Phys. Lett. B **110** (1982) 44.

[6] R. Barbieri and R. Gatto, Phys. Lett. B **110** (1982) 211.

[7] J. R. Ellis, T. Falk, G. Ganis and K. A. Olive, Phys. Rev. D **62**, 075010 (2000) [arXiv:hep-ph/0004169].

[8] J. R. Ellis, T. Falk, G. Ganis, K. A. Olive and M. Srednicki, Phys. Lett. B **510**, 236 (2001) [arXiv:hep-ph/0102098].

[9] For other recent calculations, see, for example: A. B. Lahanas, D. V. Nanopoulos and V. C. Spanos, Phys. Lett. B **518** (2001) 94 [arXiv:hep-ph/0107151]; V. Barger and C. Kao, Phys. Lett. B **518**, 117 (2001) [arXiv:hep-ph/0106189]; L. Roszkowski, R. Ruiz de Austri and T. Nihei, JHEP **0108**, 024 (2001) [arXiv:hep-ph/0106334]; A. Djouadi, M. Drees and J. L. Kneur, JHEP **0108**, 055 (2001) [arXiv:hep-ph/0107316]; H. Baer, C. Balazs and A. Belyaev, JHEP **0203**, 042 (2002) [arXiv:hep-ph/0202076].

[10] J. Ellis, T. Falk and K. A. Olive, Phys. Lett. B **444** (1998) 367 [arXiv:hep-ph/9810360]; J. Ellis, T. Falk, K. A. Olive and M. Srednicki, Astropart. Phys. **13** (2000) 181 [arXiv:hep-ph/9905481]; M. E. Gómez, G. Lazarides and C. Pallis, Phys. Rev. D **61** (2000) 123512 [arXiv:hep-ph/9907261] and Phys. Lett. B **487** (2000) 313 [arXiv:hep-ph/0004028]; R. Arnowitt, B. Dutta and Y. Santoso, Nucl. Phys. B **606** (2001) 59 [arXiv:hep-ph/0102181].

[11] C. Boehm, A. Djouadi and M. Drees, Phys. Rev. D **62** (2000) 035012 [arXiv:hep-ph/9911496]; J. Ellis, K.A. Olive and Y. Santoso, arXiv:hep-ph/0112113.

[12] V. Berezinsky, A. Bottino, J. R. Ellis, N. Fornengo, G. Mignola and S. Scopel, Astropart. Phys. **5**, 1 (1996) [arXiv:hep-ph/9508249]; P. Nath and R. Arnowitt, Phys. Rev. D **56**, 2820 (1997) [arXiv:hep-ph/9701301].

[13] M. Drees, M. M. Nojiri, D. P. Roy and Y. Yamada, Phys. Rev. D **56**, 276 (1997) [Erratum-ibid. D **64**, 039901 (1997)] [arXiv:hep-ph/9701219].

[14] J. R. Ellis, T. Falk, G. Ganis, K. A. Olive and M. Schmitt, Phys. Rev. D **58** (1998) 095002 [arXiv:hep-ph/9801445].

[15] S. Mizuta and M. Yamaguchi, Phys. Lett. B **298** (1993) 120 [arXiv:hep-ph/9208251]; J. Edsjo and P. Gondolo, Phys. Rev. D **56** (1997) 1879 [arXiv:hep-ph/9704361].

[16] M. Drees and M. M. Nojiri, Phys. Rev. D **47** (1993) 376 [arXiv:hep-ph/9207234]; H. Baer and M. Brhlik, Phys. Rev. D **53** (1996) 597 [arXiv:hep-ph/9508321] and Phys. Rev. D **57** (1998) 567 [arXiv:hep-ph/9706509]; H. Baer, M. Brhlik, M. A. Diaz, J. Ferrandis, P. Mercadante, P. Quintana and X. Tata, Phys. Rev. D **63** (2001) 015007 [arXiv:hep-ph/0005027]; A. B. Lahanas, D. V. Nanopoulos and V. C. Spanos, Mod. Phys. Lett. A **16** (2001) 1229 [arXiv:hep-ph/0009065].

[17] Joint LEP 2 Supersymmetry Working Group, *Combined LEP Chargino Results, up to 208 GeV*,
`http://lepsusy.web.cern.ch/lepsusy/www/inos_moriond01/charginos_pub.html`.

[18] Joint LEP 2 Supersymmetry Working Group, *Combined LEP Selectron/Smuon/Stau Results, 183-208 GeV*,
`http://alephwww.cern.ch/~ganis/SUSYWG/SLEP/sleptons_2k01.html`.

[19] LEP Higgs Working Group for Higgs boson searches, OPAL Collaboration, ALEPH Collaboration, DELPHI Collaboration and L3 Collaboration, *Search for the Standard Model Higgs Boson at LEP*, ALEPH-2001-066, DELPHI-2001-113, CERN-L3-NOTE-2699, OPAL-PN-479, LHWG-NOTE-2001-03, CERN-EP/2001-055, arXiv:hep-ex/0107029; *Searches for the neutral Higgs bosons of the MSSM: Preliminary combined results using LEP data collected at energies up to 209 GeV*, LHWG-NOTE-2001-04, ALEPH-2001-057, DELPHI-2001-114, L3-NOTE-2700, OPAL-TN-699, arXiv:hep-ex/0107030.

[20] Y. Okada, M. Yamaguchi and T. Yanagida, Prog. Theor. Phys. **85** (1991) 1; J. R. Ellis, G. Ridolfi and F. Zwirner, Phys. Lett. B **257** (1991) 83; H. E. Haber and R. Hempfling, Phys. Rev. Lett. **66** (1991) 1815.

[21] S. Heinemeyer, W. Hollik and G. Weiglein, Comput. Phys. Commun. **124** (2000) 76 [arXiv:hep-ph/9812320]; S. Heinemeyer, W. Hollik and G. Weiglein, Eur. Phys. J. C **9** (1999) 343 [arXiv:hep-ph/9812472].

[22] M.S. Alam et al., [CLEO Collaboration], Phys. Rev. Lett. **74** (1995) 2885 as updated in S. Ahmed et al., CLEO CONF 99-10; BELLE Collaboration, BELLE-CONF-0003, contribution to the 30th International conference on High-Energy Physics, Osaka, 2000. See also K. Abe *et al.*, [Belle Collaboration], [arXiv:hep-ex/0107065]; L. Lista [BaBar Collaboration], [arXiv:hep-ex/0110010]; C. Degrassi, P. Gambino and G. F. Giudice, JHEP **0012** (2000) 009 [arXiv:hep-ph/0009337]; M. Carena, D. Garcia, U. Nierste and C. E. Wagner, Phys. Lett. B **499** (2001) 141 [arXiv:hep-ph/0010003]. D. A. Demir and K. A. Olive, Phys. Rev. D **65**, 034007 (2002) [arXiv:hep-ph/0107329].

[23] K. Chetyrkin, M. Misiak and M. Munz, Phys. Lett. B **400**, 206 (1997) [Erratum-ibid. B **425**, 414 (1997)] [hep-ph/9612313]; T. Hurth, hep-ph/0106050;

[24] H. N. Brown *et al.* [Muon g-2 Collaboration], Phys. Rev. Lett. **86**, 2227 (2001) [arXiv:hep-ex/0102017].

[25] M. Knecht and A. Nyffeler, arXiv:hep-ph/0111058; M. Knecht, A. Nyffeler, M. Perrottet and E. De Rafael, Phys. Rev. Lett. **88**, 071802 (2002) [arXiv:hep-ph/0111059]; M. Hayakawa and T. Kinoshita, arXiv:hep-ph/0112102; I. Blokland, A. Czarnecki and K. Melnikov, Phys. Rev. Lett. **88**, 071803 (2002) [arXiv:hep-ph/0112117]; J. Bijnens, E. Pallante and J. Prades, Nucl. Phys. B **626**, 410 (2002) [arXiv:hep-ph/0112255].

[26] L. L. Everett, G. L. Kane, S. Rigolin and L. Wang, Phys. Rev. Lett. **86**, 3484 (2001) [arXiv:hep-ph/0102145]; J. L. Feng and K. T. Matchev, Phys. Rev. Lett. **86**, 3480 (2001) [arXiv:hep-ph/0102146]; E. A. Baltz and P. Gondolo, Phys. Rev. Lett. **86**, 5004 (2001) [arXiv:hep-ph/0102147]; U. Chattopadhyay and P. Nath, Phys. Rev. Lett. **86**, 5854 (2001) [arXiv:hep-ph/0102157]; S. Komine, T. Moroi and M. Yamaguchi, Phys. Lett. B **506**, 93 (2001) [arXiv:hep-ph/0102204]; J. Ellis, D. V. Nanopoulos and K. A. Olive, Phys. Lett. B **508** (2001) 65 [arXiv:hep-ph/0102331]; R. Arnowitt, B. Dutta, B. Hu and Y. Santoso, Phys. Lett. B **505** (2001) 177 [arXiv:hep-ph/0102344] S. P. Martin and J. D. Wells, Phys. Rev. D **64**, 035003 (2001) [arXiv:hep-ph/0103067]; H. Baer, C. Balazs, J. Ferrandis and X. Tata, Phys. Rev. D **64**, 035004 (2001) [arXiv:hep-ph/0103280].

[27] J. R. Ellis, K. A. Olive and Y. Santoso, arXiv:hep-ph/0202110.

[28] A. Melchiorri and J. Silk, arXiv:astro-ph/0203200.

[29] J. L. Feng, K. T. Matchev and T. Moroi, Phys. Rev. Lett. **84**, 2322 (2000) [arXiv:hep-ph/9908309]; J. L. Feng, K. T. Matchev and T. Moroi, Phys. Rev. D **61**, 075005 (2000) [arXiv:hep-ph/9909334]; J. L. Feng, K. T. Matchev and F. Wilczek, Phys. Lett. B **482**, 388 (2000) [arXiv:hep-ph/0004043].

[30] T. Falk, K. A. Olive, L. Roszkowski and M. Srednicki, Phys. Lett. B **367**, 183 (1996) [arXiv:hep-ph/9510308]; T. Falk, K. A. Olive, L. Roszkowski, A. Singh and M. Srednicki, Phys. Lett. B **396**, 50 (1997) [arXiv:hep-ph/9611325].

[31] M. Battaglia *et al.*, Eur. Phys. J. C **22**, 535 (2001) [arXiv:hep-ph/0106204]; J. R. Ellis, J. L. Feng, A. Ferstl, K. T. Matchev and K. A. Olive, arXiv:astro-ph/0110225.

[32] M. Carena, S. Heinemeyer, C. E. Wagner and G. Weiglein, arXiv:hep-ph/0202167.